Journal of Organometallic Chemistry 694 (2009) 3688–3691

Contents lists available at ScienceDirect

Journal of Organometallic Chemistry

journal homepage: www.elsevier.com/locate/jorganchem

Communication

Excited-state absorption of *mono*-, *di*- and *tri*-nuclear cyclometalated platinum 4,6-diphenyl-2,2′-bipyridyl complexes

Yunjing Li [a], Timothy M. Pritchett [b], Pin Shao [a], Joy E. Haley [c,d], Hongjun Zhu [a], Wenfang Sun [a,*]

[a] Department of Chemistry and Molecular Biology, North Dakota State University, Fargo, ND 58108-6050, USA
[b] U.S. Army Research Laboratory, AMSRD-ARL-SE-EM, 2800 Powder Mill Road, Adelphi, MD 20783-1197, USA
[c] Materials and Manufacturing Directorate, Air Force Research Laboratory, Wright Patterson Air Force Base, OH 45433, USA
[d] UES Inc., Dayton, OH 45432, USA

ARTICLE INFO

Article history:
Received 11 May 2009
Received in revised form 28 July 2009
Accepted 29 July 2009
Available online 6 August 2009

Keywords:
Triplet excited-state absorption cross-section
Singlet excited-state absorption cross-section
Excited-state lifetime
Triplet quantum yield
Cyclometalated platinum(II) 4,6-diphenyl-2,2′-bipyridyl complexes
Z-scan

ABSTRACT

The ground-state absorption cross-sections (σ_g), triplet excited-state absorption cross-section (σ_T) at 532 nm, singlet excited-state absorption cross-sections (σ_s) at various visible wavelengths, singlet and triplet excited-state lifetimes, and triplet quantum yields of three cyclometalated platinum(II) 4,6-diphenyl-2,2′-bipyridyl complexes, are reported. The presence of metal–metal and π–π interactions in the dinuclear and trinuclear complexes results in a significant increase in their respective σ_g's in the visible spectral region. As a result, the ratio of σ_s/σ_g and σ_T/σ_g at each wavelength is significantly greater for the mononuclear complex than for the dinuclear and the trinuclear complexes.

The photophysics of cyclometalated platinum(II) complexes has attracted considerable attention in recent years because of the potential applications of these materials in photocatalysis [1], light emitting devices [2,3], and chemical sensors [4,5]. Nonlinear optical studies conducted by our group indicate that platinum terdentate complexes exhibit broad and relatively strong triplet excited-state absorption in the visible to near-IR spectral region, making them promising candidates for photonic devices that require strong excited-state absorption [6]. The dinuclear platinum(II) 4,6-diphenyl-2,2′-bipyridyl complex with bis(diphenylphosphino)methane bridging ligand ((dphbpyPt)$_2$dppm, **2**), and the trinuclear platinum(II) 4,6-diphenyl-2,2′-bipyridyl complex with bis(diphenylphosphinomethyl)phenylphosphine bridging ligand ((dphbpyPt)$_3$dpmp, **3**) were recently synthesized and investigated by our group (Fig. 1) [7,8]. Complex **2** was found to exhibit stronger nonlinear transmission than the corresponding mononuclear platinum(II) 4,6-diphenyl-2,2′-bipyridyl triphenylphosphine complex (dphbpyPtPPh$_3$, **1**) [7], and this could be attributed to the intramolecular π–π interactions between the two 4,6-diphenyl-2,2′-bipyridine ligands. On the other hand, the addition of a third metal center in **3** results in an increase of the ground-state absorption in the visible spectral region, which leads to a weaker nonlinear transmission [8]. To gain greater insight into the manner in which these intramolecular interactions influence the optical nonlinearities observed in these platinum complexes, we carried out the nanosecond and picosecond Z-scan measurements on acetonitrile solutions of **1**–**3**. The Z-scan data were fitted by a five-level model, making use of independently measured values for the singlet and triplet excited-state lifetimes and of the triplet quantum yield. The values of the singlet exited-state absorption cross-section and the triplet excited-state absorption cross-section are reported in this paper. Finally, the causes underlying the observed differences are analyzed.

The synthesis and structural characterization of **1**–**3** have been reported previously [7,8]. Fig. 2 shows the UV–Vis absorption spectra of **1**–**3** in acetonitrile solution. All complexes exhibit intense absorption below 400 nm, which is attributed to the π,π* transition of the 4,6-diphenyl-2,2′-bipyridine ligand(s). The shoulder at approximately 425 nm is attributed to the ^{1}MLCT (metal-to-ligand charge transfer) transition. In comparison to **1**, a broad and weak absorption band is observed in the region of 475–600 nm for **2** and **3**. This band can be assigned to the ^{1}MMLCT (metal–metal-to-ligand charge transfer) transition due to Pt–Pt interactions

* Corresponding author. Tel.: +1 701 2316254; fax: +1 701 2318831.
E-mail address: Wenfang.Sun@ndsu.edu (W. Sun).

0022-328X/$ - see front matter © 2009 Elsevier B.V. All rights reserved.
doi:10.1016/j.jorganchem.2009.07.045

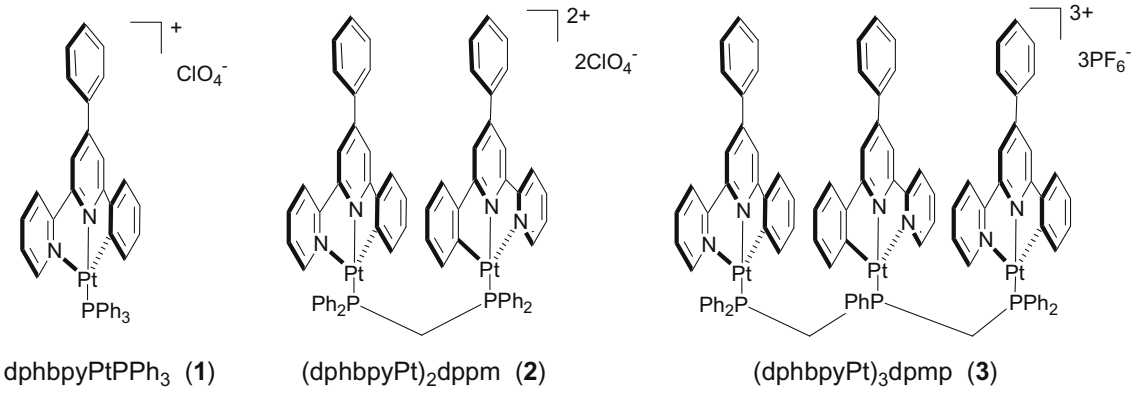

Fig. 1. Chemical structures of $dphbpyPtPPh_3$ (**1**), $(dphbpyPt)_2dppm$ (**2**), and $(dphbpyPt)_3dpmp$ (**3**) complexes.

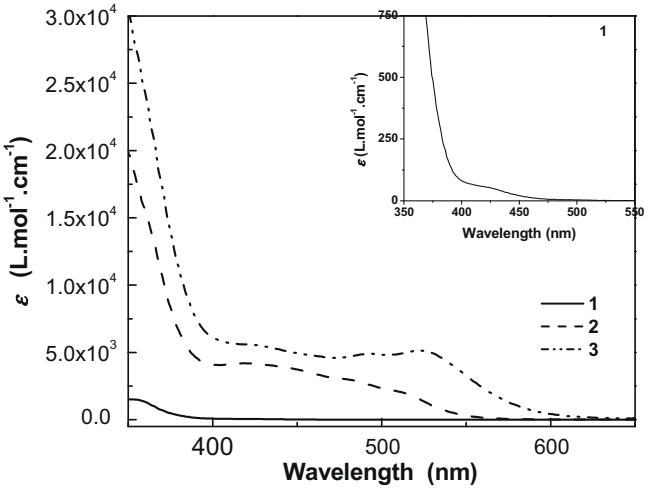

Fig. 2. UV–Vis spectra of **1**–**3** in CH_3CN. The inset shows the expansion of the spectrum for **1**.

[7,8]. The ^{1}MMLCT band is red-shifted from 475–550 nm for **2** to 475–600 nm for **3**, indicating a stronger metal–metal interaction in the trinuclear complex than that in the dinuclear complex. At the same time, the molar extinction coefficient (or, equivalently, the ground-state absorption cross-section) at a fixed wavelength increases as one moves from the mononuclear to the trinuclear platinum complex. In addition, **1**, **2** and **3** are essentially transparent at wavelengths above 450 nm, 550 nm and 600 nm, respectively. In each complex, this provides a broad optical window from the visible to the near-infrared region in which the excited-state absorption cross-section is higher than the ground-state absorption cross-section. This latter observation has been validated by the nanosecond transient difference absorption (TA) spectra previously reported by our group for **1**–**3** [7,8] and will be further verified by the fs transient difference absorption measurements and the Z-scan experiments described below.

Our previous ns TA study shows that **1**–**3** all exhibit a broad, positive absorption band from 370 nm to 820 nm [7,8]. The band maximum is red-shifted from 540 nm for **1** to 590 nm for **2**, and 600 nm for **3**. This trend is in line with that observed in the UV–Vis absorption spectra and is attributed to the increased strength of intramolecular π–π and metal–metal interactions moving from the mononuclear to the dinuclear and trinuclear complexes. In this work, the triplet excited-state extinction coefficient ($\varepsilon_{T_1-T_n}$) and the quantum yield of triplet excited-state formation (Φ_T) for each complex were determined using the partial saturation method [9], in which the optical density at the respective T_1–T_n absorption band maximum for each complex was monitored when the excitation energy at 355 nm was gradually increased. The experimental data was then fitted using the following equation to obtain the ε_T and Φ_T [9]

$$\Delta OD = a(1 - \exp(-bI_p)) \quad (1)$$

where ΔOD is the optical density at the monitored wavelength, I_p is the pump intensity in Einstein cm^{-2}, $a = (\varepsilon_T - \varepsilon_0)dl$, and $b = 2303\varepsilon_0^{ex}\Phi_T/A$. ε_T and ε_0 are the absorption coefficients of the excited state and the ground state at the monitored wavelength, ε_0^{ex} is the ground-state absorption coefficient at the excitation wavelength of 355 nm, d is the concentration of the sample (mol L^{-1}), l is the thickness of the sample, and A is the area of the sample irradiated by the excitation beam. The experimental data and the fitting curve are presented in Fig. 3 for **2** and **3**; and the resultant values of $\varepsilon_{T_1-T_n}$ (540 nm) = 4292 M^{-1} cm^{-1} and Φ_T = 0.23 for **1**, $\varepsilon_{T_1-T_n}$ (590 nm) = 3100 M^{-1} cm^{-1} and Φ_T = 0.25 for **2**, and $\varepsilon_{T_1-T_n}$ (600 nm) = 6240 M^{-1} cm^{-1} and Φ_T = 0.12 for **3** are listed in Table 1.

In order to evaluate the excited-state absorption in a shorter time regime, femtosecond transient absorption measurements were performed using a femtosecond pump–probe UV–Vis spectrometer (HELIOS) manufactured by Ultrafast Systems LLC. Each sample was excited at 390 nm with a 170 fs Ti:sapphire laser pulse (Clark-MXR CPA 2010, 1 kHz repetition rate, 1 mJ/pulse at 780 nm), and the absorption was probed from 450 to 750 nm with white light continuum. The results for **1** and **3** are presented in Fig. 4. For **1**, a small peak around 530 nm with a short-lived transient appears first and then grows rapidly into a long-lived transient. Both the spectrum and the lifetime of the long-lived transient are consistent with those measured by the ns laser flash photolysis spectrometer [7], suggesting that the newly formed transient is the triplet excited state and that the growth of the triplet excited state occurs in a very short time. Fitting the femtosecond transient absorption decay data yields a singlet excited-state lifetime of τ_{S1} = 8.9 ± 1.7 ps, while fitting the nanosecond transient absorption decay data gives a triplet excited-state lifetime of τ_{T1} = 127 ± 3 ns [7]. The features of the fs transient difference absorption spectra of **2** and **3** are both broader and slightly stronger than that of **1**, with the band maximum appearing at 600 nm and 650 nm for **2** and **3**, respectively. In line with what has been observed in **1**, one observes a short-lived transient followed by a long-lived transient in both **2** and **3**. The spectra corresponding to the long-lived transients are essentially consistent with the respective ns transient difference absorption spectra reported by our group previously [7,8], and thus are tentatively attributed to the triplet excited-state absorption. The singlet and triplet excited-state lifetimes deduced from the decay of the fs and ns transients are

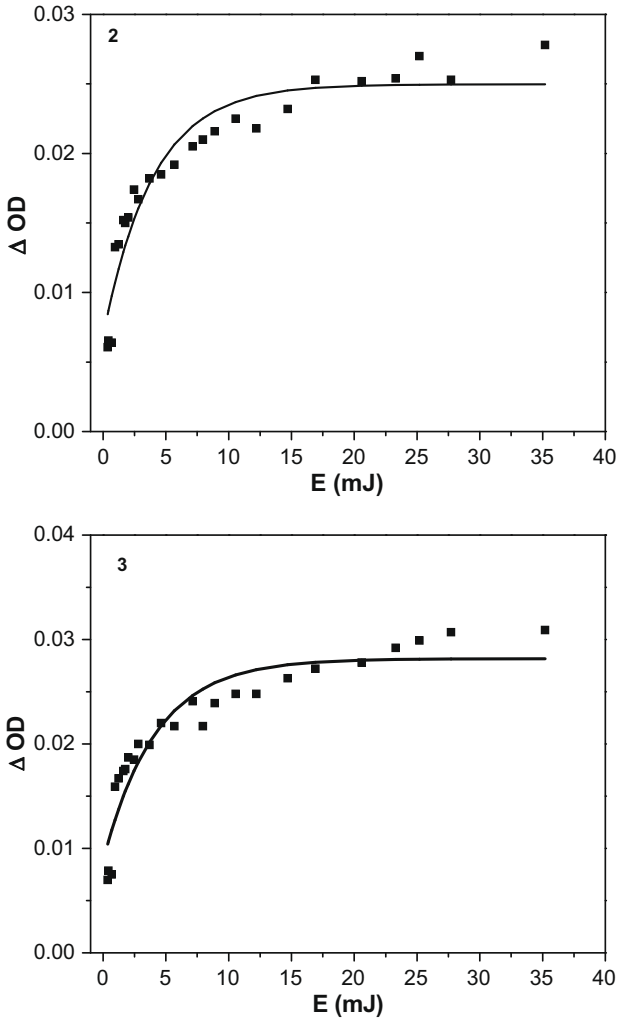

Fig. 3. Optical density of ns transient absorption of **2** at 590 nm and **3** at 600 nm vs. excitation energy. The squares represent the experimental data, and the solid lines are the fitting results.

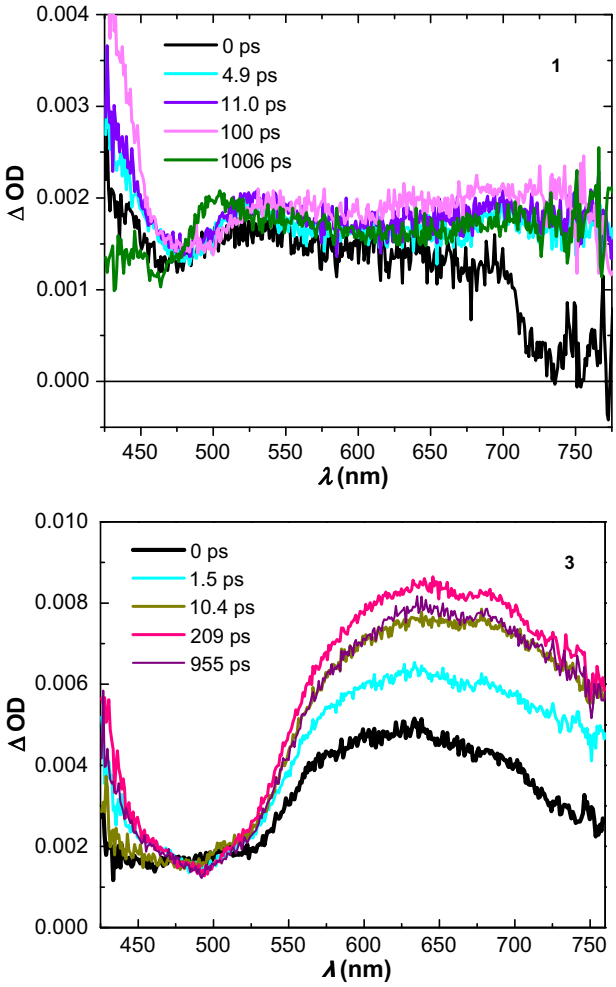

Fig. 4. Time-resolved fs transient difference absorption spectra of **1** and **3** in CH_3CN.

Table 1
Photophysical parameters of **1**–**3** in CH_3CN.

	τ_S/ps	τ_T/ns	Φ_T	$\lambda_{T_1-T_n}$/nm $\varepsilon_{T_1-T_n}$/l mol^{-1} cm^{-1})	τ_{isc}/ps[a]
1	8.9 ± 1.7	127 ± 3	0.23	540 (4292)	38.7
2	3.2 ± 1.0	184 ± 9	0.25	590 (3100)	12.8
3	8.9 ± 2.8	588 ± 23	0.12	600 (6240)	74.2

[a] $\tau_{isc} = \tau_s/\Phi_T$.

3.2 ± 1.0 ps and 184 ± 9 ns, respectively, for **2**, and 8.9 ± 2.8 ps and 588 ± 23 ns for **3**. The intersystem crossing times ($\tau_{isc} = \tau_s/\Phi_T$) are then calculated to be 39 ps for **1**, 13 ps for **2,** and 74 ps for **3**. Since these intersystem crossing times are of the same magnitude as the pulsewidth of the ps laser (21 ps) used for the Z-scan measurements, both the singlet and triplet excited states contribute to the observed ps Z-scan signal, whereas the ns Z scan is dominated by the triplet excited state.

To quantitatively compare the excited-state absorption characteristics of **1**–**3**, open-aperture Z-scan experiments of **1** in DMSO and **2** and **3** in CH_3CN were performed using both nanosecond and picosecond laser pulses. For the nanosecond Z-scan measurements, a Quantel Brilliant Nd:YAG laser operating at its second-harmonic output (532 nm) with a 10 Hz repetition rate was used as the light source. The laser pulse was focused to a 36 μm spot located at the center of a 1-mm cell. The picosecond Z scans employed an EKSPLA PG 401 picosecond optical parametric generator (OPG) pumped by the third harmonic of an EKSPLA PL 2143A Nd:YAG laser with a pulsewidth of 21 ps and a repetition rate of 10 Hz. The output of the OPG was adjusted to selected wavelengths in the range of 475–600 nm. The spatial profile of the beam was nearly Gaussian after a spatial filter. The beam waist ω_0 varied from 30 μm to 37 μm over the range of 475–600 nm. All beam radii (HW/e^2) were measured using a knife edge. The picosecond Z scans were performed in a 2-mm sample cell.

Fig. 5 shows the typical open-aperture Z-scan results exemplified by **2** using ns and ps laser pulses at 532 nm. The experimental Z-scan data were analyzed using a five-band model that incorporated experimentally measured values of the singlet excited-state lifetime, the triplet excited-state lifetime, the triplet quantum yield, and the ground-state absorption cross-section [10]. For each complex at 532 nm, a single pair of excited-state absorption cross-section values (σ_S, σ_T) was obtained by simultaneously fitting both the ns and ps Z scans. (Here, σ_S and σ_T denote, respectively, the absorption cross-sections of the lowest lying singlet excited state and of the lowest lying triplet state.) In fitting ps Z scans at wavelengths other than 532 nm, the value of σ_T was estimated from the value at 532 nm that was obtained from simultaneous fitting of the corresponding 532-nm Z scans and the ratio of the optical density change at 532 nm and at each respective wavelength according to the ns transient absorption spectrum at zero time delay [9,11]. The solid curves in Fig. 5 represent the best fit of the experimental

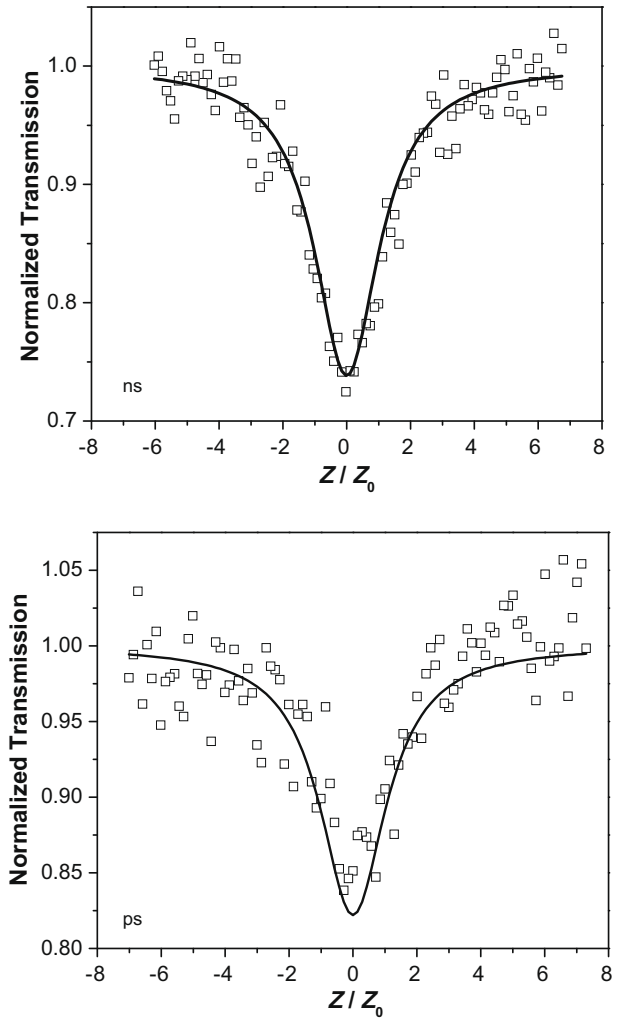

Fig. 5. Normalized open-aperture Z-scan data (open squares) and fitting curves (solid lines) for **2** at 532 nm.

Z-scan data for **2** and correspond to the values of $\sigma_S = 1 \times 10^{-18}$ cm^2 and $\sigma_T = 5.0 \times 10^{-17}$ cm^2, or, equivalently, to the ratios of $\sigma_S/\sigma_g = 0.5$ and $\sigma_T/\sigma_g = 25$ at 532 nm. Although in **2** σ_S is smaller than σ_g at 532 nm, rapid intersystem crossing allows for significant triplet excited-state absorption even at ps time scales; the fact that σ_T is considerably larger than σ_g at 532 nm then leads to an effective excited-state absorption cross-section that is much larger than that of the ground state. Consequently, reverse saturable absorption is observed in **2** in both the ns and ps measurements. Using the estimated σ_T-values at wavelengths of 550 nm and 570 nm, the following values of σ_S were obtained by fitting the relevant ps Z-scans of **2**: 4.5×10^{-17} cm^2 (550 nm) and 7.0×10^{-17} cm^2 (570 nm). The values (σ_S, σ_T) for **1** and **3** at various wavelengths are listed in Table 2.

Comparing the σ_S and σ_g values at different wavelengths for each complex, one observes that σ_S generally increases at longer wavelengths, while the σ_g decreases at longer wavelengths. This results in an increased ratio of σ_S/σ_g at a longer wavelength for each complex. Therefore, stronger reverse saturable absorption is expected at longer wavelengths for each complex. Moreover, at each wavelength probed, the ratios of σ_S/σ_g and σ_T/σ_g increase dramatically moving from **3** to **1**. This is a result of the increased excited-state absorption and decreased ground-state absorption at each respective wavelength from **3** to **1**. Since intramolecular metal–metal interactions are enhanced going from the mononuclear complex **1** to the trinuclear complex **3**, we conclude that metal–metal interactions disfavor the excited-state absorption and consequently reduce the reverse saturable absorption.

Table 2
Wavelength-dispersion of excited-state absorption cross-sections of **1**–**3** in CH_3CN.

	λ/nm	$\sigma_g/10^{-19}$ cm^2	$\sigma_s/10^{-18}$ cm^2	σ_s/σ_g	$\sigma_T/10^{-18}$ cm^2	σ_T/σ_g
1	475	2.68	60	224	6	22.4
	500	1.45	40	276	6.2	42.8
	532	0.22	60	2727	6.5	295
	550	0.15	110	7333	7	467
2	532	20.3	1	0.5	50	24.6
	550	7.2	45	62.5	60	83.3
	570	3.4	70	206	69	203
3	532	64.7	–	–	30	4.64
	550	43.7	18	4.12	45	10.3
	570	21.6	35	16.2	58	26.9
	600	12.8	40	31.3	68	53.1

In summary, the lifetime of the singlet excited state, the lifetime of the triplet excited state, and the triplet quantum yield were measured for **1**–**3**. Based on these values, the triplet excited-state absorption cross-section at 532 nm and singlet excited-state absorption cross-sections at various wavelengths were obtained by using a five-level dynamic model to fit open-aperture Z scans in nanosecond and picosecond regimes. The ratios of the excited-state to ground-state absorption cross-sections are found to vary dramatically at different wavelengths and for different complexes. The presence of intramolecular metal–metal interactions significantly decreases the excited-state absorption cross-section but increases the ground-state absorption. As a result, the mononuclear complex **1** displays the highest ratio of σ_S/σ_g and σ_T/σ_g, while the trinuclear complex **3** exhibits the lowest ratio at each respective wavelength.

Acknowledgments

W. Sun acknowledges the financial support from the NSF (CAREER CHE-0449598) and the Army Research Laboratory (W911NF-06-2-0032).

References

[1] A.R. Dick, J.W. Kampf, M.S. Sanford, Organometallics 24 (2005) 482.
[2] W.-Y. Wong, Z. He, S.-K. So, K.-L. Tong, Z. Lin, Organometallics 24 (2005) 4079.
[3] W. Lu, B.X. Mi, M.C.W. Chan, Z. Hui, C.M. Che, N. Zhu, S.T. Lee, J. Am. Chem. Soc. 126 (2004) 4958.
[4] S.C.F. Kui, S.S.-Y. Chui, C.-M. Che, N. Zhu, J. Am. Chem. Soc. 128 (2006) 8297.
[5] K.M.-C. Wong, W.-S. Tang, X.-X Lu, N. Zhu, V.W.-W. Yam, Inorg. Chem. 44 (2005) 1492.
[6] W. Sun, Z.-X. Wu, Q.-Z. Yang, L.-Z. Wu, C.-H. Tung, Appl. Phys. Lett. 82 (2003) 850.
[7] W. Sun, H. Zhu, P.M. Barron, Chem. Mater. 18 (2006) 2602.
[8] P. Shao, W. Sun, Inorg. Chem. 46 (2007) 8603.
[9] I. Carmichael, G.L. Hug, J. Phys. Chem. Ref. Data 15 (1986) 1.
[10] Y. Li, T.M. Pritchett, J. Huang, M. Ke, P. Shao, W. Sun, J. Phys. Chem. A 112 (2008) 7200.
[11] P. Shao, Y. Li, W. Sun, Organometallics 27 (2008) 2743.